EUCAS23-3-LP-CD-04S

Cryogenic test stand for characterization of magnetocaloric materials

Carlos Hernando, Javier Munilla, Luis García-Tabarés, Juan Carlos del Real, Iván Castro, Luis González, Fernando Toral

***Abstract*— Alternative cryogenic refrigeration methods are needed to improve the low efficiency of traditional gas cycles cryocoolers. Magnetic refrigeration is an old known technique used to reach below Kelvin temperatures, though there is rising interest in using this method at liquid helium and liquid hydrogen temperatures due to its high Carnot efficiency. However, further experimentation is needed to fully understand the heat transfer dynamics of magnetocaloric materials at cryogenic temperatures. A test stand has been designed to evaluate the heat transfer coefficients of these materials using the single-blow transient test technique. The system consists of a hermetic helium gas circuit, which is cooled down to cryogenic temperatures and is forced to flow through a packed bed of magnetocaloric material. In order to test the heat transfer properties of the magnetocaloric materials at different magnetic fields the test stand has a superconducting solenoid capable of providing up to 4 T. The design and validation of the test stand for the characterization of magnetocaloric materials is described in the present paper.**

***Index Terms*— Cryogenics, Magnetic refrigeration, Magnetocaloric effect, cryogenic system, experimental analysis.**

I. INTRODUCTION

APPLICATIONS requiring refrigeration are numerous and wide-ranging. The cooling temperature needed in each application ranges from temperatures of 300 K (ambient temperature) to almost absolute zero (liquid helium). Among the latter, superconducting applications stand out, as they need temperatures of few Kelvins to achieve the superconducting state. For the refrigeration of these systems, devices called cryocoolers are commonly used [1], [2].

Cryocoolers have undergone major advances in the last 20 years, improving their heat rejection capacity, and reliability. However, the cost and Carnot efficiency of these devices are still limiting factors [3] for the development of breakthrough superconducting applications. Therefore, alternative refrigeration methods are being continuously explored. Magnetic refrigeration is a promising alternative, since the reversible nature of the undergone process delivers high Carnot efficiencies [4]. The magnetocaloric effect (or MCE) [5], is the basis of magnetic refrigeration.

For the modelling of a magnetic refrigerator, it is essential to establish the heat transfer and fluid dynamics mechanisms. Typically, correlations used for ambient temperature processes are used [6], which have provided good results for temperatures as low as 70 K [7]. However, there is a limited literature on the validation of heat transfer and fluid dynamics correlations at liquid helium temperature. The most comprehensive work is found in [8], but the conclusions are not definitive since large fluctuation in the measured temperatures were observed.

This article presents the design of a test station for the characterization and heat transfer analysis of magnetocaloric materials down to liquid Helium (LHe) temperature based on the single-blow technique. The system has a superconducting magnet capable of providing up to 4 T.

II. EXPERIMENTAL APPARATUS

The single-blow technique is a transient method which allows to measure the heat transfer coefficient of a heat exchanger. This procedure requires a constant flow rate through the test bed and a step-wise fluid flow inlet temperature change.

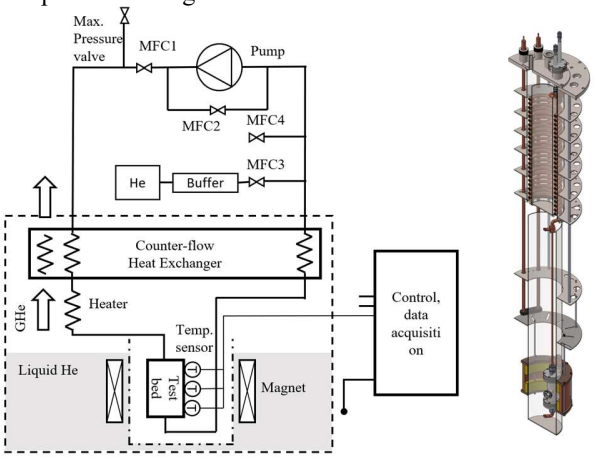

Fig. 1 Schematic of apparatus and data acquisition system. The portion enclosed by dashed lines are inside a cryostat, which is shown at the right side of the figure.

Fig. 1 shows the schematic of the experimental system. It is a closed system which uses a pump to circulate the helium through the circuit. The pressure and mass flow of the system are controlled with two mass flow controllers (MFC), MFC1 and MFC2 in Fig. 1.

The helium gas goes inside a cryostat and is cooled down in a double counterflow heat exchanger, rejecting heat to the

This work was supported by the Community of Madrid under contract IND2020/IND-17516. (Corresponding author: Carlos Hernando López de Toledo)

Carlos Hernando, and Ivan Castro are with CYCLOMED TECHNOLOGIES, Madrid, Spain and Carlos Hernando also with Comillas Pontifical University, Madrid, Spain (e-mail: c.hernando@cyclomed.tech).

Luis García-Tabarés, Javier Munilla Luis González, and Fernando Toral are with Centro de Investigaciones Energéticas, Medioambientales y Tecnológicas (CIEMAT), Madrid, Spain and Javier Munilla also with Comillas Pontifical University, Madrid, Spain.

Juan Carlos del Real with Comillas Pontifical University, Madrid, Spain.

outgoing helium gas, and to the evaporated helium from the liquid helium bath where the magnet is submerged. A heater controls the temperature at the inlet of the regenerator.

A. Magnetocaloric Material (MCM)

Inside the test bed there is the magnetocaloric material, crushed into particles of small diameter (less than 1 mm.), positioned in a packed bed as depicted in Fig. 2. Two MCMs have been selected: Gadolinium Gallium Garnet, GGG or $Gd_3Ga_5O_{12}$, and Erbium Aluminum (II), $ErAl_2$.

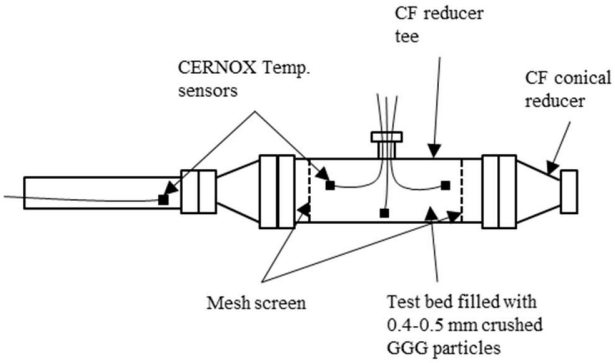

Fig. 2 Schematic of instrumented GGG packed bed.

The selection of the MCM obeys to the following rules [9]: the selection of a suitable Curie temperature, intensity of the magnetocaloric effect, high electrical resistivity (to prevent eddy currents), good manufacturing, and corrosion properties and low price.

GGG, is an antiferromagnetic material, which has been the most employed magnetic refrigerant for cryogenic applications, as its low Néel temperature (2 K), gives this material great versatility for LHe applications. Fig. 3 shows the significant entropy change near LHe boiling temperature.

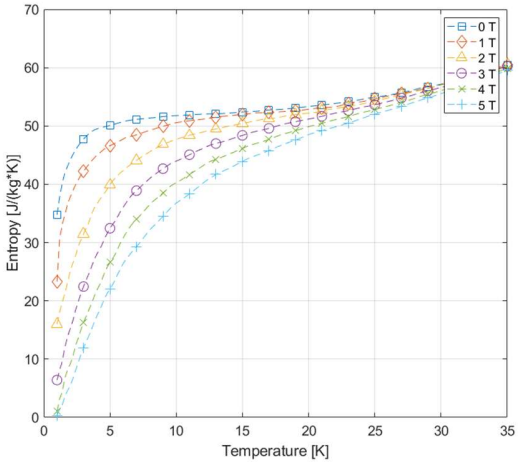

Fig. 3. Entropy of GGG with temperature and magnetic field.

On the other hand, $ErAl_2$ was selected since there are additional applications at slightly higher temperatures, like hydrogen liquefaction, that have sparked interest in recent years [10]. $ErAl_2$ is a ferromagnetic material, with a Curie temperature of 13.4 K. A ferromagnetic transition can be slightly appreciated in Fig. 4. Its optimum refrigerant capacity is theoretically higher than any other type of material.

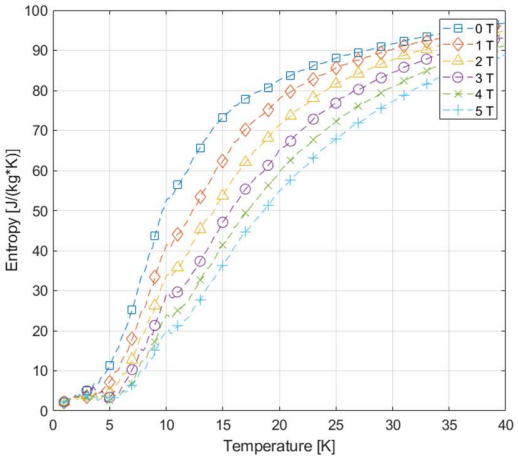

Fig. 4. Entropy of $ErAl_2$ with temperature and magnetic field.

The MCE properties of the magnetocaloric materials, as well as the quantity of material to be used in the tests, provides the boundary conditions for the rest of the components of the test stand: the magnetic source and heat transfer system, which are summarized in TABLE I.

TABLE I
RANGE OF VALUES FOR TEST STAND COMPONENT VARIABLES

Magnetic Source (Parameter)	Values
Magnetic volume	Volume: Φ40 x 100 mm
Magnetic field	> 4 T
Heat transfer circuit (Parameter)	**Values**
Temperature	6-20 K
Mass Flow	5-50 g/min

B. Magnetic Source

For a full evaluation of the material properties a magnetic field of 4 T was established, the best option is to use a superconducting magnet.

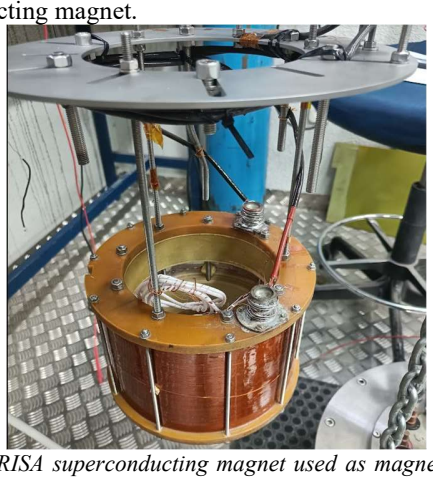

Fig. 5 CRISA superconducting magnet used as magnetic source in magnetocaloric test stand.

The magnet used in this test station, shown in Fig. 5, was developed for the CRISA project. During CRISA the power source of the antimatter spectrometer (AMS) experiment, a particle detector for the international space station (ISS), was tested [11]. Its characteristics are summarized in TABLE II.

TABLE II

MAIN ELECTROMAGNETIC PROPERTIES OF CRISA MAGNET

Parameter	Value
Superconducting Material	NbTi
Operating Temperature	4.2 K
Nominal current	450 A
Critical current	~ 600 A
Superconductor Field nominal (critical)	5.89 T (7.7 T)
Centre Field nominal (critical)	4.25 T (5.88 T)
Inductance	0.56 H
Inner bore	Φ180 x 125 mm

C. *Heat transfer circuit*

Helium gas flowing through the regenerator will act as the heat transfer medium. The helium is pumped from ambient temperature, which provides a more precise control of helium mass flow and pressure. The equipment used is summarized in TABLE III.

TABLE III
HELIUM CIRCUIT PUMPING COMPONENTS

Equipment	Model
Mechanical Pump	KNF Diaphragm Gas Pump N 630.1.2
Mass flow controllers	Voegtlin mass flow controllers

Gas helium will also be responsible for cooling down the magnetocaloric material down to near its Curie (or Néel) temperature, where the MCE effect is more significant. For this purpose, a cryogenic heat exchanger was developed to recover the enthalpy of the evaporated Helium from the liquid bath which is cooling the superconducting magnet.

This cryogenic heat exchanger is similar to a Giauque-Hampson heat exchanger [12], although in this case there is an additional heat recovery stage. The helium that exits the packed bed, flows inside the incoming helium circuit to increase the test station efficiency. The schematic of the heat exchanger is shown in Fig. 6. To control the temperature at the inlet of the regenerator a heater is placed immediately at the exit of the heat exchanger.

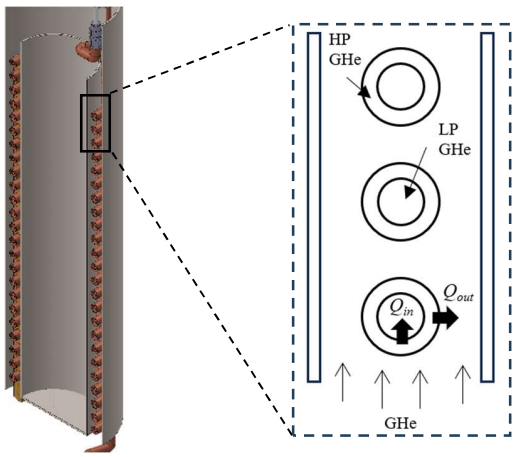

Fig. 6 Cryogenic heat exchanger for MC test stand (left), detailed view of the cross section of the heat exchanger, showing the heat transfer (Q_{in}) from the high pressure helium gas (HP GHe) to the evaporated helium gas, and the heat transfer (Q_{out}) to the low pressure helium gas (LP GHe) (right).

III. COMPONENTS DESIGN AND VALIDATION

A. *Magnetocaloric Material: Preparation and validation*

For the construction of a packed bed regenerator, the procedure followed described in [6],[13] was adopted:

1. Pre-crush the magnetocaloric material crystals to the required size. To achieve the chosen size the crushed crystals are passed through a series of sieves of unique dimensions. Fig. 7 shows a sample of crushed $ErAl_2$.
2. Fill the regenerator with the crushed crystals and apply certain packing pressure to achieve the chosen porosity, defined as the relation between the void volume and the total volume of the packed bed.

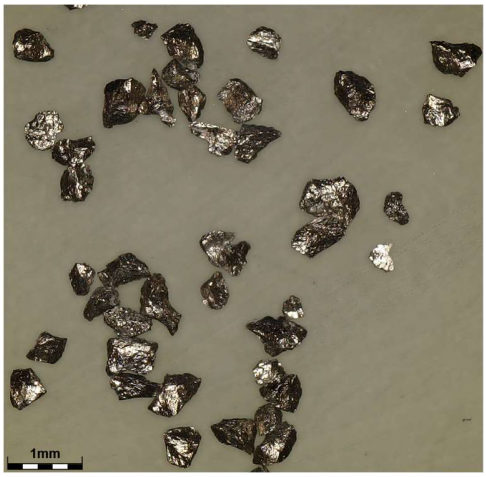

Fig. 7 Crushed particles of $ErAl_2$ (average size of 0.45-0.55 mm.)

Ideally, the porosity of the regenerator should be minimized and therefore the packing pressure should be as high as possible. However, if the packing pressure is too high certain regions of the regenerator can become occluded, impeding the flow and isolating that region of the regenerator. Fig. 8 shows theoretical and experimental pressure drop for different porosities, it can be observed how with porosities greater than 0.45, the regenerator becomes occluded, as there is a divergence between the theoretical, given by Ergun correlation [14], and experimental pressure drop.

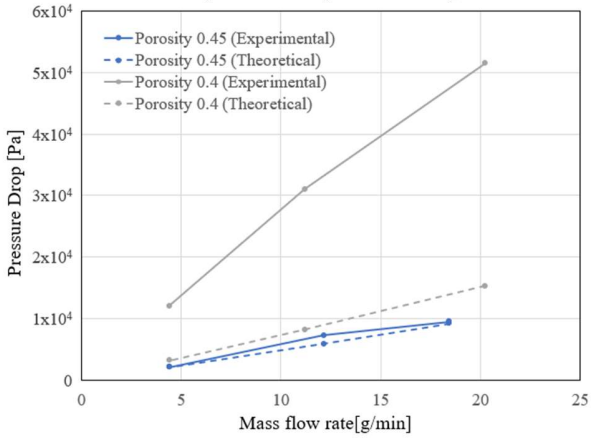

Fig. 8 Pressure drop for different porosity (packing pressures) of the regenerator.

One more parameter is needed for the characterization of the regenerator, the shape factor (ϕ). The shape factor describes the 'irregularity' of the particles, it is defined as the ratio of the specific area of a spherical particle to the specific area of the particle in question. The geometric parameters and values used in the analysis are presented in TABLE IV.

TABLE IV
TYPICAL REGENERATOR VALUES

Independent Parameter	Value
MC mass	0.1-1 kg
Regenerator Diameter	20-40 mm
Particle Diameter	0.3-0.5 mm
Porosity	0.35-0.42
Shape Factor	0.5-0.6

B. *Superconducting Magnet tests*

The superconducting magnet was manufactured in the early 2000s, therefore, there was certain probability that its superconducting properties have been degraded. Consequently, the magnet was tested alone at ambient temperature, with electrical and magnetic measurements. And at cryogenic temperatures to test the instrumentation, quench protection system, and the power source.

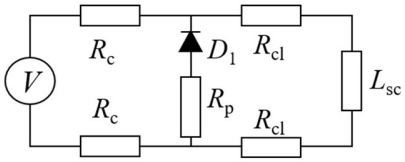

Value	
R_c	0.1 Ω
R_{cl}	30-50 mΩ
L_{sc}	0.56 H
R_p	0.08 Ω
2xD_1	I_c = 300 A V_f =2.5V

Fig. 9 Schematic and values of electrical circuit

Fig. 9 shows the schematic adopted for the cryogenic tests, where R_c is the ambient cables resistance, R_{cl} the current lead resistance, L_{sc} the inductance of the superconducting magnet, R_p is the dump resistor for quench protection, and D_1 is the protection diode, defined by its nominal current I_c, and the forward voltage V_f. Fig. 10 shows retraining from the magnet before achieving its nominal current, as it quenched during the first test at 312 A, probably due to the long time out of operation. Detection and quench system behaved as expected.

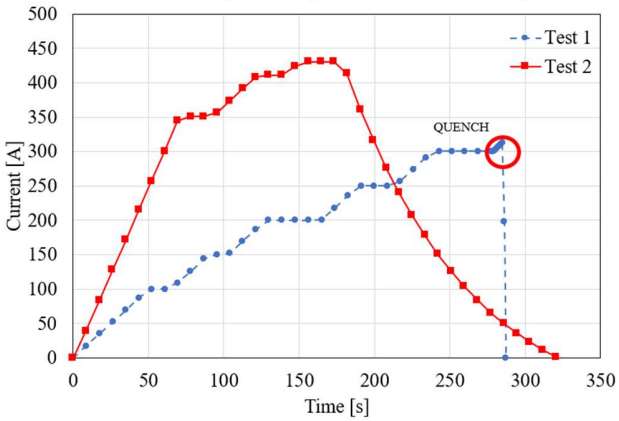

Fig. 10 Current ramp-up during training.

C. *Heat transfer circuit*

To cool down the magnetocaloric material down to its operating temperature we use the double counterflow heat exchanger, being the heat flux, Q, in each direction:

$$Q = h * (T_{f,annular} - T_{f,(int.,ext)})$$

where h is the heat transfer coefficient, $T_{f,annular}$ the hot fluid temperature, flowing through the annulus, and $T_{f,(int.,ext)}$ the cold fluid temperature, which could be the returning gas, or the evaporated helium gas. To model the heat transfer, and define the heat exchanger main parameters, the correlations shown in TABLE V are used.

TABLE V
CORRELATIONS FOR EXTERNAL AND INTERNAL FORCED CONVECTION

External flow	Equation
	$Nu = CRe^{-n}$

Re Range	C	n
0.1-4	0.989	0.67
4-40	0.911	0.615
40-4000	0.683	0.534
4000-40000	0.193	0.382
40000-400000	0.027	0.195

Internal flow	Equation
Laminar flow (Re < 2300)	$Nu_{lam} = 3.657$
Turbulent flow (Re > 10000)	$if\ \left(\frac{e}{D}\right)Re < 5 \quad Nu_t = 0.023Re^{0.8}Pr^{\frac{1}{3}}$ (Smooth pipe) $if\ \left(\frac{e}{D}\right)Re > 5 \quad Nu_{turb} = \frac{\frac{RePr^{\frac{1}{3}}f}{8}}{1+1.27\left(\frac{f}{8}\right)^{\frac{1}{2}}(Pr^{\frac{2}{3}}-1)}\left[1-\frac{1000}{Re}\right]Pr^{\frac{2}{3}}$ (Rough pipe)
Transition zone	$Nu_{tran} = (1-\lambda)Nu_{lam} + \lambda Nu_{turb}$ $\lambda = 3u^2 - 2u^3;\ u = \frac{Re-2300}{10000-2300}$

[1] Nu, is the Nusselt number, Re is the Reynolds number, Pr is the Prandlt number, e is the surface roughness of the pipe, D is the hydraulic diameter of the pipe, and f is the friction coefficient. Subscripts lam, $turb$, and $tran$ of Nu indicate laminar flow, turbulent flow, and transition zone, respectively.

Based on these correlations the heat exchanger was designed. TABLE VI shows the main dimensions.

TABLE VI
THERMAL DESIGN VALUES FOR THE COUNTERFLOW HEAT EXCHANGER

Parameter	Outer Pipe	Inner Pipe
Pipe Diameter	12 mm.	6 mm.
Pipe Width	1 mm.	1 mm.
Temperature range	293-10 K	8-267 K
Pressure Drop	50 mbar	40 mbar
Pipe length	10.25 m	
Effectiveness	91%	
Pipe Material	Copper	
Diameter & Height	150 mm x 250 mm	

IV. CONCLUSION

Magnetic refrigeration is considered to have the potential to increase the efficiency of current state of the art cryocoolers increasing their competitiveness. In this paper we presented the design and validation of a test stand to understand and characterize the thermal behavior of magnetocaloric materials at cryogenic temperatures, which will allow the development of optimized magnetic refrigerators. The system components are currently being manufactured, and the first results are expected to be obtained in the following months.

REFERENCES

[1] V. S. Chakravarthy, R. K. Shah, and G. Venkatarathnam, "A review of refrigeration methods in the temperature range 4-300 K," *J. Therm. Sci. Eng. Appl.*, vol. 3, no. 2, Jul. 2011, doi: 10.1115/1.4003701.

[2] R. Radebaugh, "Refrigeration for Superconductors," in *Proceedings of the IEEE*, Institute of Electrical and Electronics Engineers Inc., 2004, pp. 1719–1734. doi: 10.1109/JPROC.2004.833678.

[3] R. Radebaugh, "Cryocoolers: the state of the art and recent developments," *J. Phys. Condens. Matter*, vol. 21, no. 16, p. 164219, 2009, doi: 10.1088/0953-8984/21/16/164219.

[4] V. Franco, J. S. Blázquez, J. J. Ipus, J. Y. Law, L. M. Moreno-Ramírez, and A. Conde, "Magnetocaloric effect: From materials research to refrigeration devices," *Progress in Materials Science*, vol. 93. Elsevier Ltd, pp. 112–232, Apr. 01, 2018. doi: 10.1016/j.pmatsci.2017.10.005.

[5] E. Brück, "Developments in magnetocaloric refrigeration," *Journal of Physics D: Applied Physics*, vol. 38, no. 23. IOP Publishing, p. R381, Dec. 07, 2005. doi: 10.1088/0022-3727/38/23/R01.

[6] Gregory F. Nellis, "Magnetically aumented cryogenic refrigeration," University of Wisconsin (Doctoral thesis), 1992. [Online]. Available: https://dspace.mit.edu/handle/1721.1/11482

[7] R. Morgan, C. Rota, E. Pike-Wilson, T. Gardhouse, and C. Quinn, "The modelling and experimental validation of a cryogenic packed bed regenerator for liquid air energy storage applications," *Energies*, vol. 13, no. 19, 2020, doi: 10.3390/en13195155.

[8] J. A. Barclay, W. C. Overton, W. F. Stewart, and Sunil Sarangi, "Experiment to determine properties of packed beds and regenerators at cryogenic temperatures," *Adv. Cryog. Eng.*, vol. 29, pp. 605–612, 1984, doi: 10.1007/978-1-4613-9865-3_69.

[9] A. Kitanovski, J. Tušek, U. Tomc, U. Plaznik, M. Ožbolt, and A. Poredoš, "Magnetocaloric Energy Conversion," *Green Energy Technol.*, vol. 179, no. Mcm, pp. 167–210, 2015, doi: 10.1007/978-3-319-08741-2.

[10] T. Numazawa, K. Kamiya, T. Utaki, and K. Matsumoto, "Magnetic refrigerator for hydrogen liquefaction," *Cryogenics (Guildf).*, vol. 62, pp. 185–192, Jul. 2014, doi: 10.1016/J.CRYOGENICS.2014.03.016.

[11] R. Battiston, "The antimatter spectrometer (AMS-02): A particle physics detector in space," *Nucl. Instruments Methods Phys. Res. Sect. A Accel. Spectrometers, Detect. Assoc. Equip.*, vol. 588, no. 1–2, pp. 227–234, Apr. 2008, doi: 10.1016/J.NIMA.2008.01.044.

[12] Randall F. Barron, *Cryogenic Systems*. Oxford University Press, 1985.

[13] F. K. M. C. M. Gunderson, G. F. Nellis, "The Development of an Active Magnetic Regenerative Refrigerator (AMRR) for Sub-Kelvin Cooling of Space Science Instrumentation," *Cryogenics (Guildf).*, vol. 21.

[14] S. Ergun, "Fluid Flow Through Packed Columns," *Chem. Eng. Prog.*, vol. 48, p. 89, 1952.